^{18}F Protection Issues: Human and γ-Camera Considerations

ZongJian Cao, PhD; James H. Corley, MS; and Jerry Allison, PhD

Department of Radiology, Medical College of Georgia, Augusta, Georgia

Objective: Two main issues in protecting radiation workers and the general public from ^{18}F radiation—distance from and lead shielding for an ^{18}F source—were investigated. We also examined the effect of an ^{18}F source on the counting rate of a neighboring γ-camera.

Methods: The dose rates of an ^{18}F vial and a water-filled cylinder were measured using an ionization chamber at different distances with or without lead shielding. In addition, the counting rates of γ-cameras in the presence of the ^{18}F cylinder were measured with different detector orientations, distances, and energy windows.

Results: The dose rate of a point or an extended source in air was proportional to the inverse square of the distance from the source. At 2 m, the dose rate for a 370-MBq ^{18}F source was less than 20 μGy in any single hour, which is the limit for unrestricted areas. The dose rate with 0.318-cm-thick lead shielding decreased to about 60%, and that with 5.08-cm-thick lead shielding decreased to about 4%; these rates were higher than those estimated using the narrow-beam attenuation formula. The scattered photons and characteristic x-rays from the lead brick and surrounding structures may have contributed to this result. The decrease in dose rate resulting from a 33% increase in distance was similar to the effect from shielding the source with 0.318-cm-thick lead. At 3 m from a 185-MBq ^{18}F source, the counting rate in the ^{99m}Tc window of an Orbiter camera was about 120,000/min when the detector faced the source. This rate was comparable to that of a typical ^{99m}Tc clinical study (~200,000/min). Only when the distance was increased to 11 m and the detector did not face the source did the counting rate decrease to the background level (3,234/min). The counting rate also depended on the energy window of the γ-camera. On a Vertex camera, the counting rate of ^{18}F in the ^{99m}Tc window versus that in the ^{201}Tl (or ^{67}Ga) window was 1:1.7 (or 1:2.7).

Conclusion: ^{18}F dose rate can be significantly reduced with distance. Lead shielding is not as effective as was predicted. ^{18}F sources should be kept substantial distances away from γ-cameras to avoid contamination of image quality.

For correspondence or reprints contact: ZongJian Cao, PhD, Department of Radiology, Medical College of Georgia, 1120 15th St., Augusta, GA 30912.

E-mail: zcao@mail.mcg.edu

In PET, two 511-keV photons are produced in each annihilation and are detected coincidentally by the PET scanner. Because 2 photons result from a single decay, as opposed to the 1 photon produced by conventional nuclear medicine agents, PET studies can significantly increase radiation exposure to radiation workers, other hospital staff, and the general public. More radiation protection may be needed in the design of a PET suite: for example, in determining the size of the patient-injection room, PET scanner room, and radioactive-material storage area and whether they need lead shielding. We should pay particular attention to the injection area, because activity in the patient is highest during the first hour after injection.

The effect of lead shielding on the dose rate is sometimes estimated using the transmission factor of the photon beam intensity (*1*):

$$I = I_0 e^{-\mu d}, \qquad \text{Eq. 1}$$

where I and I_0 are the intensity of the transmitted and incident beams, respectively; μ, the attenuation coefficient of the absorber; and d, the thickness of the absorber. Use of the narrow-beam attenuation coefficient to determine the transmission factor for various thicknesses of lead shielding does not account for the effect of scattered photons and characteristic lead x-rays. One approach to incorporate the effect of scattered photons and characteristic lead x-rays is to simulate them using the Monte Carlo approach. The attenuation coefficient thus determined is more accurate than the narrow-beam attenuation coefficient (*2*). However, Monte Carlo simulation demands heavy computation and often is not feasible practically. Another reported study attempted to incorporate what is termed "in-shield scattering or buildup" through use of a computational approach (*3*). The approach is efficient computationally. However, it is not clear whether the computational approach includes characteristic lead x-rays in addition to scattered photons. To incorporate the effect of scattered photons and char-

acteristic lead x-rays, an empiric buildup factor, B, is introduced into the narrow-beam attenuation equation:

$$I = B \, I_0 \, e^{-\mu d}. \qquad \text{Eq. 2}$$

The buildup factor depends on the composition and thickness of the absorber and on the incident photon energy as well. With 511-keV photons, the buildup factor is approximately 1.13 for 0.318-cm-thick lead and 2.15 for 5.08-cm-thick lead.

In this study, we measured dose rates from ^{18}F sources for different distances and thicknesses of lead shielding. Compared with transmission factor estimates based on the narrow-beam attenuation formula or the more sophisticated Monte Carlo simulation and computational approach, dose rate measurements are more accurate because no assumptions or simplifications are involved.

When PET procedures are performed within or adjacent to a conventional nuclear medicine department, the 511-keV photons, the associated scattered radiation, and the characteristic lead x-rays can contribute unwanted counts to γ-cameras designed for studies using lower-energy photons. Thus, counts from ^{18}F sources can potentially affect image quality on γ-cameras, resulting in reduced image contrast. In this study, we investigated the importance of this phenomenon.

MATERIALS AND METHODS

We measured the exposure rates of a glass vial that initially contained 792 MBq of [18]F (as a point source) and a cylindric phantom (diameter, 20 cm; height, 20 cm) filled with water that initially contained 392 MBq of [18]F (as an extended source) in air using an ionization chamber that had a sensitive volume of 180 cm[3] and a diameter of 8 cm. Exposure rates were measured at 12 source-to-detector distances: 0.1, 0.5, 1.0, 1.5, 2.0, 2.5, 3.0, 3.5, 4.0, 4.5, 5.0, and 5.5 m. For the cylinder, the source-to-detector distances were measured from the central axis of the cylinder. The purpose of using the cylinder was to determine how well the exposure rate of an extended source followed the inverse-square law and how much the exposure rate of an extended source differed from that of a point source.

We then investigated the effect of lead shielding on the exposure rate. The ^{18}F vial was placed close to a 60-cm (width) × 12-cm (height) × 0.318-cm (thickness) lead sheet or a 20-cm (width) × 10-cm (height) × 5.08-cm (thickness) lead brick as shown in Figure 1. The vial was elevated to prevent radiation leakage from the bottom of the lead shield. To simulate the most possible shielding design in practice (lead shielding only in the wall), no lead shielding was used above or below the vial. Exposure rates were measured on the other side of the lead shield at 0.5, 1.0, 1.5, 2.0, 2.5, 3.0, 3.5, 4.0, 4.5, 5.0, and 5.5 m from the source. The experiment took place in a large conference room, and to reduce the scatter effect, no lead (or other heavy metal) structures were around.

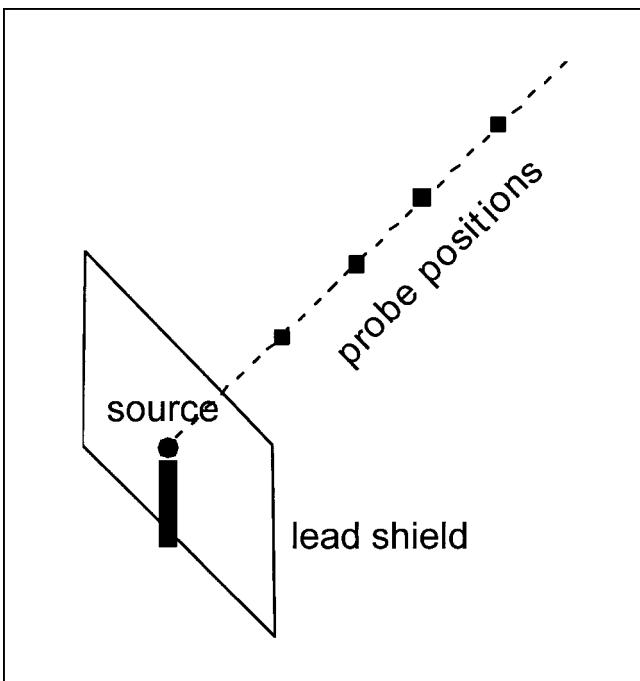To study the effect of ^{18}F source distance on the counting

FIGURE 1. Experimental setup. [18]F source was placed directly behind lead shield. Dose rates were measured on other side of lead shield at different distances from source using high-pressure ionization chamber.

rate of a nearby γ-camera, we used an Orbiter camera (Siemens Medical Systems, Inc.) to acquire counts for 1 min with the ^{18}F cylinder placed 3, 7.5, or 11 m from the camera. The camera had a round detector with a diameter of 36 cm and a thickness of 0.95 cm and was equipped with a low-energy all-purpose collimator (LEAP) (Siemens). The energy window was set for [99m]Tc (140% ± 10% keV). At a 3-m source-to-detector distance, acquisition was performed for 3 detector orientations: facing the ^{18}F cylinder, facing the floor, and facing away from the ^{18}F cylinder. At 7.5 and 11 m, counts were acquired only with the detector facing the ^{18}F cylinder. For each distance and detector orientation, 3 consecutive acquisitions were performed and then the acquired counts were averaged.

To examine the dependence of ^{18}F counting rate on the energy window of a γ-camera, we measured counting rates on a Vertex camera (ADAC Laboratories) for 3 isotope energy windows: [99m]Tc (140% ± 10% keV), [201]Tl (70% ± 10% keV plus 167% ± 10% keV), and [67]Ga (93% ± 10% keV plus 185% ± 10% keV plus 296% ± 10% keV). The ^{18}F cylinder was placed 4 m from the camera. The 2 rectangular detectors of the Vertex camera have dimensions of 50 × 40 cm and a thickness of 0.95 cm. They were equipped with LEAP collimators (ADAC). Three detector orientations for each energy window were studied: facing the ^{18}F cylinder, facing the floor, and facing away from the ^{18}F cylinder.

For all measurements, time was recorded and physical decay of ^{18}F activity was corrected. The dose rates were normalized to 370 MBq, and the γ-camera counting rates were normalized to 185 MBq. The ionization chamber mea-

sured exposure rates (mR/h). The conversion ratio between exposure rate and dose rate in air was 0.87, which is approximately 1, so we have 1 mR/h ≈ 1 mrad/h ≈ 10 μGy/h. In the following, we use the term *dose rate* with a unit of μGy/h/370 MBq and the term *counting rate* with a unit of count/min/185 MBq. Dose rates and counting rates for any other activities can be linearly scaled from the results given by this study.

RESULTS

Vial Versus Cylinder Dose Rate in Air

The dose rates of the ^{18}F vial and cylinder decreased as the distance from the source was increased (Table 1). We used an inverse-square function to fit the data points (excluding the 0.1-m data point) in Figure 2 and obtained the following result:

$$(\text{dose rate})_{\text{vial}} = \frac{0.154}{d^2} \, \mu\text{Gy/h/MBq and (dose rate)}_{\text{cylinder}}$$

$$= \frac{0.102}{d^2} \, \mu\text{Gy/h/MBq.} \qquad \text{Eq. 3}$$

Here, the distance d is in meters. The results indicate that the dose rates of both point source (vial) and extended source (cylinder) followed the inverse square law when the distance was greater than 0.5 m. If one takes 226 μGy/h/370 MBq at 0.5 m as the base, the inverse-square law predicts 56.5 μGy/h/370 MBq (10.7% smaller than the measured 63.3 μGy/h/370 MBq) at 1 m, 14.1 μGy/h/370 MBq (close to the measured 14.3 μGy/h/370 MBq) at 2 m, 6.27 μGy/h/370 MBq (close to the measured 6.25 μGy/h/370 MBq) at 3 m, 3.53 μGy/h/370 MBq (10.2% smaller than the measured 3.93 μGy/h/370 MBq) at 4 m, and 2.26 μGy/h/370 MBq (11.4% smaller than the measured 2.55 μGy/h/370 MBq) at 5 m. Because of the logarithm scale of the dose rate, the same deviation appears smaller in the plot when the dose rate is high. The deviation may have been caused by the relatively large detector size. Despite the deviation be-
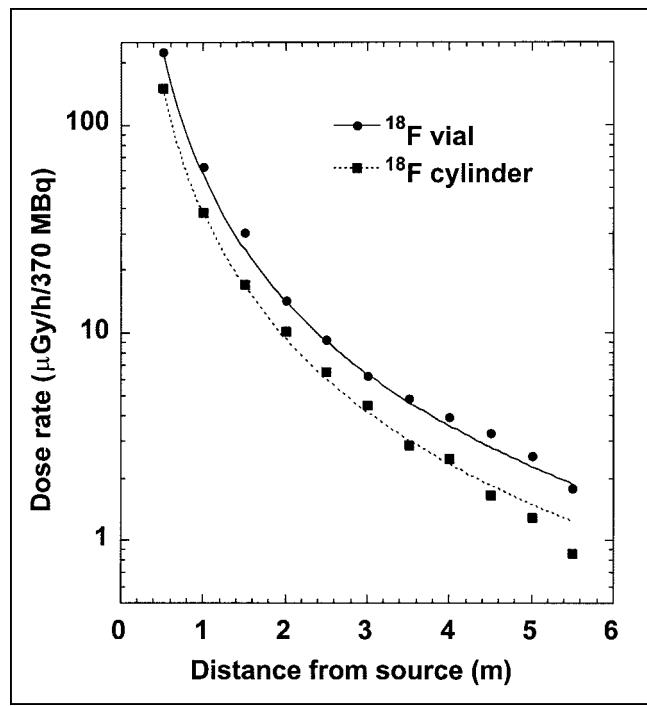

FIGURE 2. Dose rates of ^{18}F vial (● and solid curve) and cylinder (■ and dashed curve) in air as function of distance. Both curves were obtained by fitting to data points using inverse square function. Fitting result is given in Equation 3.

tween the calculated and measured dose rates, the γ-constant obtained from the fitting (0.154 μGy/h/MBq at 1 m) agreed well with the value quoted in the literature for a 511-keV photon point source in air (1,541 μGy/h/MBq at 1 cm) (*2*).

In-Air Versus Lead-Shielded Dose Rate

The dose rate of the ^{18}F vial decreased to about 60% when the vial was shielded with 0.318-cm-thick lead and to less than 4% when shielded with 5.08-cm-thick lead (Table 2). The dose rate with 0.318-cm-thick lead shielding approximately followed the inverse-square law, because a large portion of the dose rate was contributed by penetrating primary photons. The dose rate with 5.08-cm-thick lead shielding decreased with increasing distance but failed to follow the inverse-square law because of the contribution of scatter from the edges of the lead brick and surrounding structures. The dose rate eventually decreased to the background level when the distance was beyond 2 m.

Measured Versus Calculated Dose Rate for Lead-Shielded ^{18}F Source

The measured dose rates with lead shielding (Tables 3 and 4), in particular with 5.08-cm-thick lead, were higher than the values calculated using the attenuation formula (Eq. 1) with the narrow-beam attenuation coefficient (1.70/cm for 511-keV photons in lead). With 0.318-cm-thick lead, the average ratio of the measured dose rate to the calculated dose rate was 1.07, which is in approximate agreement with the buildup factor (1.13) quoted in the

TABLE 1
Dose Rates of ^{18}F Vial and ^{18}F Cylinder in Air

Distance (m)	Vial dose rate (μGy/h/370 MBq)	Cylinder dose rate (μGy/h/370 MBq)	Cylinder/vial dose-rate ratio
0.10	3,686	2,662	0.72
0.50	226	150	0.66
1.00	63.3	38.0	0.60
1.50	30.5	17.2	0.56
2.00	14.3	10.1	0.71
2.50	9.32	6.50	0.70
3.00	6.25	4.51	0.72
3.50	4.85	2.90	0.60
4.00	3.93	2.47	0.63
4.50	3.27	1.67	0.51
5.00	2.55	1.29	0.51
5.50	1.80	0.86	0.48

TABLE 2
Dose Rates of ^{18}F Vial in Air and Shielded with 0.318 or 5.08-cm-Thick Lead

Distance (m)	Dose rate in air (μGy/h/370 MBq)	0.318-cm lead shielding		5.08-cm lead shielding	
		Dose rate (μGy/h/370 MBq)	Lead/in-air dose-rate ratio	Dose rate (μGy/h/370 MBq)	Lead/in-air dose-rate ratio
0.50	226	136	0.60	4.53	0.020
1.00	63.3	35.0	0.55	2.48	0.039
1.50	30.5	15.9	0.52	1.39	0.046
2.00	14.3	8.99	0.63	0.56	0.039
2.50	9.32	5.44	0.58		
3.00	6.25	4.06	0.65		
3.50	4.85	2.95	0.61		
4.00	3.93	2.34	0.60		
4.50	3.27	1.76	0.54		
5.00	2.55	1.19	0.47		

literature (4). With 5.08-cm-thick lead, however, the ratio varied from 112 (at 0.5 m) to 311 (at 1.5 m), which are much higher values than the value quoted in the literature (2.15). The cause may have been the detection of more scatter photons, not included in the literature value, from the edges of the lead brick and surrounding structures. Inaccuracy in measuring low dose rates may also have contributed to the deviation.

Effect of ^{18}F Source on Counting Rate of Nearby γ-Camera

The counting rate measured in the ^{99m}Tc window (140% ± 10% keV) on an Orbiter camera whose detector faced an ^{18}F cylinder 3 m away was 122,487/min/185 MBq (Table 5). This counting rate was comparable with that of a typical ^{99m}Tc clinical study (~200,000/min) on the same camera. In Table 6 we see another example. The counting rate in the ^{99m}Tc window on a Vertex camera when the detector faced the ^{18}F cylinder was about 150,000/min/185 MBq, which was comparable with the counting rate of a typical ^{99m}Tc clinical study (from 150,000/min to 300,000/min) on that camera. The ^{18}F counts provided a uniform background in the image acquired on the γ-cameras and significantly reduced image contrast.

To reduce the ^{18}F counting rate, the source should be kept distant from the γ-camera and the detector of the γ-camera should not face the source. The counting rate of the Orbiter camera facing the ^{18}F cylinder decreased from 122,487/min/185 MBq to 24,501/min/185 MBq when the distance was increased from 3 to 7.5 m, and the rate decreased further to 13,468/min/185 MBq when the distance was increased to 11 m (Table 5). When the detector did not face the ^{18}F cylinder, it was more difficult for the high-energy photons to penetrate the thicker lead shield around the detector. Almost equal counting rates (31,671/min and 32,227/min at 3 m from a 185-MBq ^{18}F cylinder) were recorded for the Orbiter camera facing the floor and facing away from the ^{18}F cylinder. Both were still much higher than the background counting rate (3,234/min). We estimate from Table 5 that the counting rate will decrease to the background level (13,468/122,487 × 31,671 = 3,482/min) when the γ-camera is 11 m away from a 185-MBq ^{18}F cylinder and the detector does not face the source. This distance will vary for other cameras and collimators.

The counting rate from a ^{18}F source also depends on the energy window of the γ-camera. As shown in Table 6, the ^{99m}Tc counting rate was lower than that of ^{201}Tl or ^{67}Ga,

TABLE 3
Measured and Calculated Dose Rates of ^{18}F Vial Shielded with 0.318-cm-Thick Lead

Distance (m)	Measured dose rate (μGy/h/370 MBq)	Calculated dose rate* (μGy/h/370 MBq)	Measured/calculated dose-rate ratio
0.50	136	132.8	1.02
1.00	35.0	33.2	1.05
1.50	15.9	14.8	1.08
2.00	8.99	8.3	1.08
2.50	5.44	5.3	1.02
3.00	4.06	3.7	1.10
3.50	2.95	2.7	1.09
4.00	2.34	2.1	1.13
4.50	1.76	1.6	1.07
5.00	1.19	1.3	0.90

*Calculated using Equation 1 with I_0 the in-air dose rate given by Equation 3 for same distance.

TABLE 4
Measured and Calculated Dose Rates of ^{18}F Vial Shielded with 5.08-cm-Thick Lead

Distance (m)	Measured dose rate (μGy/h/370 MBq)	Calculated dose rate* (μGy/h/370 MBq)	Measured/calculated dose-rate ratio
0.50	4.53	0.0403	112
1.00	2.48	0.0101	246
1.50	1.39	0.0045	311
2.00	0.56	0.0025	222

*Calculated using Equation 1 with I_0 the in-air dose rate given by Equation 3 for same distance.

with a 1:1.7 ratio between the ^{99m}Tc and ^{201}Tl windows and a 1:2.7 ratio between the ^{99m}Tc and ^{67}Ga windows. This was because the wider ^{201}Tl and ^{67}Ga windows could acquire more scatter counts and because the 170-keV backscatter peak fell within the 167% ± 10% keV window of ^{201}Tl and the 185% ± 10% keV window of ^{67}Ga. In addition, the lead x-rays might have been counted in the ^{201}Tl 70% ± 10% keV window and the ^{67}Ga 93% ± 10% keV window.

The above results were obtained using an Orbiter camera with a Siemens LEAP collimator or a Vertex camera with ADAC LEAP collimators. The counting rate may vary with different cameras and collimator designs.

DISCUSSION

The dose rate of the cylinder was lower than that of the vial, because of photon attenuation in the water of the cylinder and extension of activity. Photon attenuation depends on the composition and dimensions of the attenuator. For the cylinder used in this study, the average decrease in dose rate was 38%. In patient studies, the decrease in dose rate can be larger but will depend on the patient's dimensions.

The dose rate 2 m from a 370-MBq ^{18}F vial was 14.3 μGy/h, which is below the limit of 20 μGy in any single hour recommended by the Nuclear Regulatory Commission for an unrestricted area. For extended sources such as a patient, the distance can be shorter.

The distance from the source played a critical role in reducing the dose rate. For example, the dose rate 2 m from a 370-MBq ^{18}F vial in air (14.3 μGy/h/370 MBq) was lower than that at 1.5 m with 0.318-cm-thick lead shielding (15.9 μGy/h/370 MBq), and the dose rate at 4 m in air (3.93 μGy/h/370 MBq) was lower than that at 3 m with 0.318-cm-thick lead shielding (4.06 μGy/h/370 MBq). Thus, in-

creasing the distance from 1.5 to 2 m or from 3 to 4 m (a 33% increase in distance) was more effective in decreasing the dose rate than was shielding the source with 0.318-cm-thick lead. In practice, a relatively small increase in the size of a patient-injection room or a PET scanner room may avoid the need to shield the walls of the room with lead (sometimes impossible because of structure restrictions).

Lead bricks 5.08 cm thick shielded a large quantity of ^{18}F. At 50 cm from a 1.63-GBq ^{18}F source shielded with 5.08-cm-thick lead, the dose rate was 20 μGy/h. If the distance is increased to 1 m (or 2 m), the activity can be increased to 2.98 GBq (or 13.2 GBq) and the dose rate kept to less than 20 μGy in any single hour.

Although some ^{18}F counts may come from scattered photons inside the patient body that have an energy near 140 keV and align with the collimator holes, the counts acquired by a γ-camera when its detector does not face the source are due to penetration of the 511-keV primary photons and high-energy scattered photons through the collimator and lead shield of the γ-camera. The penetrating photons deposit energy in the detector. If the energy is around 140 keV, the event will be counted.

Because the Vertex camera had a larger detector and thicker collimator, the counting rate for the detector facing the ^{18}F cylinder on the Vertex camera (150,583/min/185 MBq) was higher than that on the Orbiter camera (122,487/min/185 MBq). The detector of the Vertex had an area 1.88 times that of the Orbiter, but because of the thicker collimator of the Vertex, the ratio of the counting rate decreased to 1.23. When the detector did not face the ^{18}F source, the Vertex counting rates (7,125/min/185 MBq and 15,838/min/185 MBq) were lower than the Orbiter counting rates (31,671/min/185 MBq and 32,227/min/185 MBq), possibly because of the thicker lead shielding around the Vertex

TABLE 5
Counting Rates in 140-keV Window of Orbiter Camera Due to Nearby ^{18}F Cylinder

Detector-to-^{18}F source distance (m)	Counting rate when facing ^{18}F source (count/min/185 MBq)	Counting rate when facing floor (count/min/185 MBq)	Counting rate when facing away from source (count/min/185 MBq)	No source (count/min)
3.0	122,487	31,671	32,227	3,234
7.5	24,501			
11.0	13,468			

TABLE 6
Counting Rates of Vertex Camera Due to ^{18}F Cylinder

Energy window	Counting rate when facing source (count/min/185 MBq)	Counting rate when facing floor (count/min/185 MBq)	Counting rate when facing away from source (count/min/185 MBq)	No source (count/min)
^{99m}Tc	150,583	7,125	15,838	2,332
^{201}Tl	261,939	10,415	21,688	3,430
^{67}Ga	405,622	17,320	38,502	5,446

Source-to-detector distance was 4 m.

detectors. In addition, the counting rate for the Vertex detector facing the floor was only about half that for the Vertex detector facing away from the ^{18}F source. The reason may have been that the lead shielding on the side of the detector was thicker than that on the back of the detector.

CONCLUSION

This study found that distance is effective in decreasing dose rate and in protecting people from ^{18}F radiation and that lead shielding is not as effective as was predicted. Increasing the distance can avoid the need for lead shielding of walls. Although low beyond 1 m in air, dose rate affects the counting rate of nearby γ-cameras. Only when distance is increased to 11 m and the detector does not face the source does counting rate decrease to the background level. Dose rate also depends on the energy window of the γ-camera; images acquired in the ^{201}Tl and ^{67}Ga windows are more vulnerable to a nearby ^{18}F source. ^{18}F sources should be kept distant from γ-cameras to avoid contamination of image quality.

REFERENCES

1. Courtney JC, Mendez P, Hidalgo-Salvatierra O, Bujenovic S. Photon shielding for a positron emission tomography suite. *Health Phys.* 2001;81(suppl):S24–S28.
2. Kearfott KJ, Carey JE, Clemenshaw MN, Faulkner DB. Radiation protection design for a clinical positron emission tomography imaging suite. *Health Phys.* 1992;63:581–589.
3. Faulkner DB, Kearfott KJ, Manning RG. Planning a clinical PET center. *J Nucl Med Technol.* 1991;19:5–19.
4. Shleien B, Terpiak MS. *The Health Physics and Radiological Health Handbook.* Olney, MD: Nuclear Lantern Associates; 1984.